

Fermi-liquid ground state in n-type copper-oxide superconductor $\text{Pr}_{0.91}\text{LaCe}_{0.09}\text{CuO}_{4-y}$

Guo-qing Zheng¹, T. Sato¹, Y. Kitaoka¹, M. Fujita², and K. Yamada²

¹ Department of Physical Science, Graduate School of Engineering Science, Osaka University, Osaka 560-8531, Japan and

² Institute for Chemical Research, Kyoto University, Uji, Kyoto 610-0011, Japan

(Dated: November 21, 2018)

We report nuclear magnetic resonance studies on the low-doped n-type copper-oxide $\text{Pr}_{0.91}\text{LaCe}_{0.09}\text{CuO}_{4-y}$ ($T_c=24$ K) in the superconducting state and in the normal state uncovered by the application of a strong magnetic field. We find that when the superconductivity is removed, the underlying ground state is the Fermi liquid state. This result is at variance with that inferred from previous thermal conductivity measurement and contrast with that in p-type copper-oxides with a similar doping level where high- T_c superconductivity sets in within the pseudogap phase. The data in the superconducting state are consistent with the line-nodes gap model.

PACS numbers: 74.25.Jb, 74.72.Jt, 76.60.-k

The underlying ground state from which superconductivity evolves is closely related to, and may even determine, the nature of the superconductivity. In conventional metals, BCS type of superconductivity develops out of a ground state described by Landau's Fermi liquid theory in which electrons, even interact with each other, can be treated as dressed fermions called quasiparticles [1]. By contrary, the normal state above the transition temperature (T_c) in the p-type (hole-doped) copper-oxide superconductors deviates [2] from the Fermi liquid. One of the emerging pictures is that high- T_c superconductivity evolves out of a new state of matter [3]. Meanwhile, the n-type (electron-doped) copper-oxide superconductors $\text{Re}_{2-x}\text{Ce}_x\text{CuO}_{4-y}$ (Re=Nd, Pr, Eu or Sm) [4] show a substantially lower T_c than their p-type counterparts. It is therefore an outstanding important question of what is the difference in the underlying ground state between these two classes of materials. Early experiments found that the electrical conductivity in $\text{Re}_{2-x}\text{Ce}_x\text{CuO}_{4-y}$ (Re=Nd, Pr) is strikingly different from that in the p-type copper-oxides [5, 6], but it is recently suggested that the ground state in $\text{Pr}_{1.85}\text{Ce}_{0.15}\text{CuO}_{4-y}$ is a "spin-charge separated" state, as the case thought to occur in the p-type materials, where electrons have different capability to transport heat and charge [7].

In this study, we suppress superconductivity in the n-type $\text{Pr}_{0.91}\text{LaCe}_{0.09}\text{CuO}_{4-y}$ ($T_c=24$ K) with a strong magnetic field and evaluate the normal state using ^{63}Cu nuclear magnetic resonance (NMR). We find that the ground state hidden behind superconductivity is the Fermi liquid. When the superconductivity is removed, the spin lattice relaxation rate ($1/T_1$) was found to follow the $T_1T=\text{constant}$ relation, known as Korringa law [8], down to a very low temperature of $T=0.2$ K. The NMR data in the superconducting state, which were obtained for the first time in $\text{Re}_{2-x}\text{Ce}_x\text{CuO}_4$, are rather consistent with line-nodes gap model.

High quality single crystal of $\text{Pr}_{1-x}\text{Ce}_x\text{LaCuO}_{4-y}$ used in this study was grown by the traveling-solvent-floating-

zone method [9]. Here half of Pr was replaced by La that helps stabilizing crystallization to obtain large-size single crystals. More crucially, it helps eliminating the magnetic moment due to the rare earth element that has been the main cause for preventing the understanding of this class of superconductors [10, 11]. Substituting x tetravalent Ce for trivalent Pr adds x electron to the CuO_2 plane. Upon doping Ce, superconductivity appears at $x=0.09$ with T_c as high as 26 K, then T_c decreases monotonically with increasing x [9]. A crystal of $5\times 2\times 0.5$ mm³ of $\text{Pr}_{0.91}\text{LaCe}_{0.09}\text{CuO}_{4-y}$ was used for NMR and ac magnetic susceptibility measurements. Figure 1 shows the critical field necessary to destroy superconductivity, H_{c2} , determined from the ac-susceptibility measured at high frequency of $f=175$ MHz (left inset of Fig. 1). The value of $H_{c2}(T=0)$ for the magnetic field (H) applied perpendicular to the CuO_2 plane ($H \parallel c$ -axis) is estimated to be less than 10 T, indicating a substantially longer superconducting-coherence-length than that in the p-type cuprates. This low H_{c2} makes it possible to access the "normal" ground state by applying a laboratory magnetic field to suppress the superconductivity. Note that in typical p-type superconductors, the highest static field of ~ 30 T using Bitter magnets can only reduce T_c to its half value [12, 13].

Taking full advantage of the large anisotropy of H_{c2} , we study the nature of the superconductivity by applying a magnetic field of 6.2 T along the CuO_2 plane ($T_c(6.2\text{T})=19$ K) and we explore the ground state by applying a field of 15.3 T perpendicular to the plane to suppress the superconductivity. A single ^{63}Cu NMR line was observed for both $H \parallel c$ -axis and $H \parallel a$ -axis. The full width at half maximum of the linewidth at $T=300$ K is ~ 150 Oe (~ 300 Oe) at $H=6.2$ T (15.3 T) $\parallel c$ -axis and ~ 75 Oe at $H=6.2$ T $\parallel a$ -axis, which indicate that the nuclear quadrupolar frequency ν_Q is very small ($\nu_Q \leq 0.5$ MHz, if any), as the case in $\text{Nd}_{1.85}\text{Ce}_{0.15}\text{CuO}_4$ [10]. This is understood as due to electron doping into the Cu 3d-orbit whose hole is the main contribution to ν_Q [14]. The $1/T_1$ of ^{63}Cu was

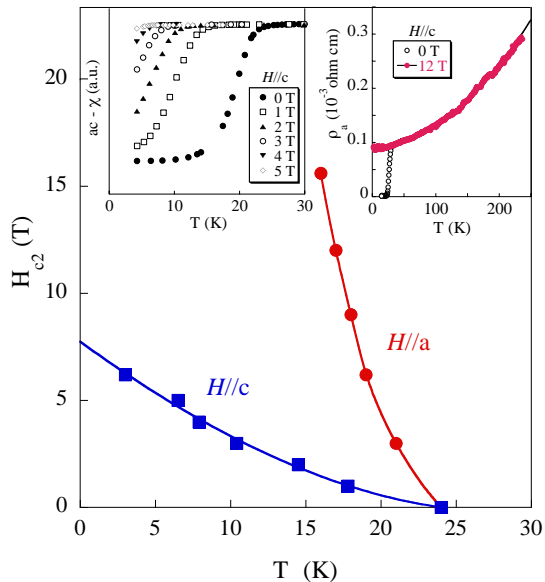


FIG. 1: The critical field of $\text{Pr}_{0.91}\text{LaCe}_{0.09}\text{CuO}_{4-y}$ as a function of temperature. The curves are guides to the eyes. The insets show the ac-susceptibility at various fields and the in-plane resistivity.

measured by the saturation-recovery method. A small RF field was used in order to avoid possible heating by the RF pulse. The value of $1/T_1$ was determined from an excellent fitting of the nuclear magnetization $M(t)$ to $\frac{M(\infty)-M(t)}{M(\infty)} = 0.1\exp(-t/T_1) + 0.9\exp(-6t/T_1)$ [15].

The key results of this study were obtained by measuring $1/T_1$ in the zero-temperature limit "normal state" when the superconductivity is suppressed. A criterion for judging an electronic state being a Fermi liquid or a "strange metal" is to see whether or not $1/T_1$ obeys the Korringa law [8]. In a Fermi liquid, those quasiparticles that participate in the nuclear spin-lattice relaxation are the quasiparticles near E_F whose population is $\sim k_B T$. Therefore $1/T_1$ is proportional to T in such a state (see below for a broader definition of the Korringa law). As seen in Fig. 2, for H along the CuO_2 plane of $\text{Pr}_{0.91}\text{LaCe}_{0.09}\text{CuO}_{4-y}$, there appears a signature of $1/T_1$ becoming proportional to T below a temperature above T_c , but only in a narrow temperature range because superconductivity sets in (see Fig. 2, circles) [16]. It is unclear whether or not this is in the middle of crossing over to a more exotic state at lower temperatures as seen in p-type cuprate superconductors. We therefore applied a strong magnetic field of 15.3 T perpendicular to the CuO_2 plane to suppress the superconductivity and thereby to reveal the ground state hidden behind the superconductivity. There, it is seen that the $T_1 T = \text{constant}$ relation indeed holds, persisting down to a very low temperature $T = 0.2$ K (also see the inset of Fig. 3). Namely, the hallmark of the Fermi liquid is unambiguously ob-

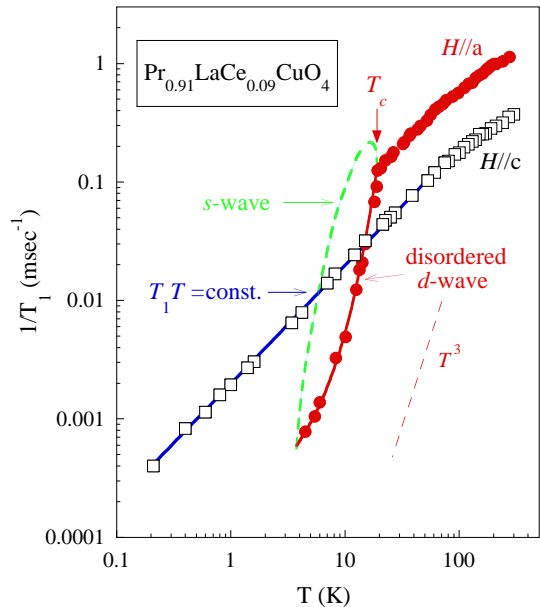


FIG. 2: Temperature dependence of the ^{63}Cu nuclear spin-lattice relaxation rate, $1/T_1$, with the magnetic field applied parallel (circles, $H = 6.2$ T) and perpendicular (squares, $H = 15.3$ T) to the CuO_2 plane, respectively. The solid curve is the calculated result for the disordered $d_{x^2-y^2}$ gap function [29], $\Delta = \Delta_0 \cos(2\theta)$, with $2\Delta_0 = 3.8k_B T_c$ and a residual DOS at the Fermi level, $N_{res} = 0.15N(E_F)$. The broken curve is the calculated result for a BCS s-wave gap, $2\Delta_0 = 3.5k_B T_c$ and the ratio of Δ_0 to the energy level breadth [30], $r = 10$.

served over more than two decades in temperature.

In order to examine in more detail how the electron-electron correlations evolve with temperature, it is instructive to plot the quantity of $1/T_1 T$ as a function of T . In Fig. 3, one sees that upon lowering temperature from 300 K, $1/T_1 T$ increases with decreasing T , but is saturated around $T = 70$ K. The most important feature is that $1/T_1 T$ becomes a constant below $T = 55$ K which persists down to $T = 0.2$ K (see the inset), as mentioned already. Note that $1/T_1 T$ probes the imaginary part of the low-frequency ($\omega \rightarrow 0$) dynamical susceptibility ($\chi(q, \omega)$) averaged over the momentum (q) space: $1/T_1 T = \frac{3k_B}{4} \frac{1}{\mu_B^2 \hbar^2} \sum_q A_q A_{-q} \frac{\chi''(q, \omega)}{\omega}$, where A_q is the hyperfine coupling constant [17]. For conventional metals described by the Fermi liquid theory, $\sum_q \chi''(q, \omega) = \pi \sum_{k, k'} \delta(E_k - E_{k'} - \hbar\omega) (f(E_{k'}) - f(E_k))$, thus one recovers the Korringa law of $1/T_1 T = \frac{\pi}{\hbar} A^2 N(E_F)^2 k_B = \frac{4\pi k_B}{\hbar} \left(\frac{\gamma_n}{\gamma_e}\right)^2 K_s^2$, where $\gamma_{e(n)}$ is the Gyromagnetic ratio of electron (nucleus) and K_s is the spin Knight shift. By contrary, when $\chi(q)$ has a peak at the antiferromagnetic wave vector $Q = (\pi, \pi)$ as seen in the p-type cuprates, $1/T_1 T$ becomes to be proportional to $\chi(Q)$ [18, 19]. The increase of $1/T_1 T$ upon decreasing temperature in $\text{Pr}_{0.91}\text{LaCe}_{0.09}\text{CuO}_{4-y}$ can therefore be attributed to the

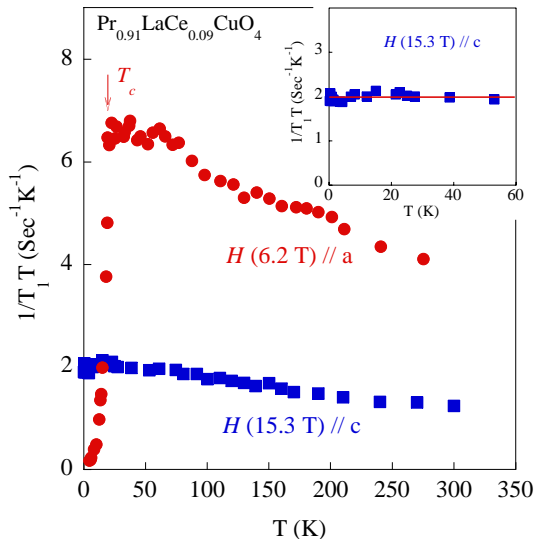


FIG. 3: The quantity of $1/T_1T$ as a function of temperature in $\text{Pr}_{0.91}\text{LaCe}_{0.09}\text{CuO}_{4-y}$. The inset emphasized the low temperature part for $H \parallel c$ -axis.

increase of $\chi(Q)$, namely, to the development of antiferromagnetic spin correlations. But the increase of $1/T_1T$ is weak, resembling that in high-doped (overdoped) p-type materials [13], which may be due to the electron-doping into the Cu-3d orbit that reduces the size of the spin moment. More importantly, for the low-doped p-type copper-oxides with carrier density usually less than 0.2, with further lowering T , $1/T_1T$ starts to decrease at a temperature T^* that is far above $T_c \sim 100$ K. This phenomenon of the loss of low-energy spectral weight or DOS is ascribed to be due to a pseudogap opening [2], which has been a subject of intensive studies over the last decade. However, the pseudogap behavior is not seen in $1/T_1T$ in $\text{Pr}_{0.91}\text{LaCe}_{0.09}\text{CuO}_{4-y}$ even though it is low-doped. Its low- T ($T \leq 55$ K) spin dynamics is renormalized to well conform to the prediction for the Fermi liquid that persists as the ground state when the superconductivity is removed.

That the present compound is a low carrier-doped sample is supported by the Knight shift result. The spin susceptibility $\chi(q=0)$ of the present sample shares a property commonly seen in low-doped p-type cuprate superconductors [20], namely, $\chi(q=0)$ decreases with lowering T , although its T_c is the highest among its class. In Fig. 4, the Knight shift, which is a sum of the orbital contribution K_{orb} and the spin contribution $K_s = A_{hf}\chi(q=0)$, are shown for both a -direction (K_a) and c -direction (K_c). K_c is less T -dependent, probably because of smaller hyperfine interaction A_{hf} in this direction, namely, K_c is predominantly orbital origin. As seen in the lower panel of Fig. 4 and the inset to it, the decrease of K_a as T is reduced ceases below $T \sim 55$ K,

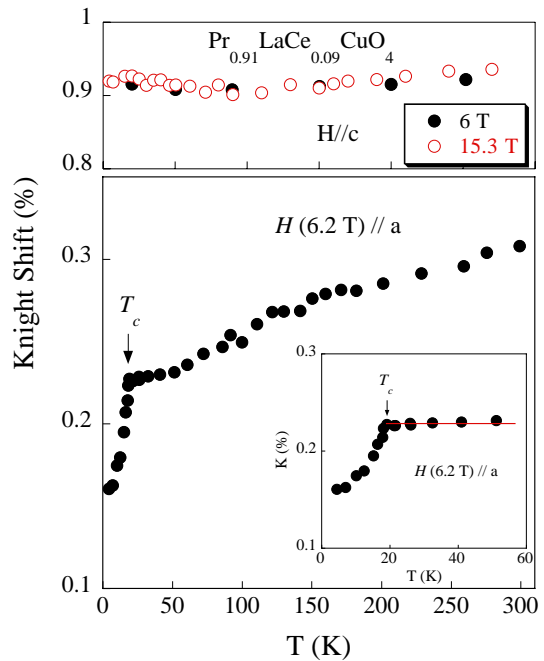


FIG. 4: Temperature dependence of the ^{63}Cu Knight shift in $\text{Pr}_{0.91}\text{LaCe}_{0.09}\text{CuO}_{4-y}$. The inset to the lower panel emphasizes the data below $T=60$ K.

namely, K_a becomes T -independent within the experimental error below $T \sim 55$ K, until superconductivity sets in. We have applied a high field of 28 T along the a -direction to reduce the T_c to ~ 10 K and confirmed that the T -independence of K_a persists down to 10 K. Thus, the criterion for the Fermi liquid in a broader sense, the requirement of $T_1TK_s^2=\text{constant}$, is also fulfilled for $T \leq 55$ K. Taking $K_{orb,a}=0.155\%$ from Fig. 4 [22], we obtain $T_1TK_s^2=7.5 \times 10^{-8}\text{Sec}\cdot\text{K}$, which is smaller by a factor of 50 than the value for non-interacting electrons of $3.75 \times 10^{-6}\text{Sec}\cdot\text{K}$. The difference primarily arises from the enhancement of $1/T_1T$ due to the antiferromagnetic spin correlation. Hence, the low- T normal state is a *strongly-correlated Landau Fermi liquid*. The in-plane resistivity ρ_a , as shown in the right inset of Fig. 1, can be fitted to $\rho_a = \rho_0 + AT^2$ with $\rho_0=92\mu\Omega\text{cm}$ and $A=3.75 \times 10^{-3}\mu\Omega\text{cmK}^{-2}$, which is consistent with such Fermi liquid state but inconsistent with other liquids [21]. Our conclusion is different from that inferred from a recent low- T thermal conductivity measurement that suggested a break-down of the Fermi liquid theory in the n-type $\text{Pr}_{1.85}\text{Ce}_{0.15}\text{CuO}_4$ [7]. Also note that in p-type cuprates, the pseudogap persists in the H -induced normal state below $T_c(H=0)$ [12, 23]. Thus, our results suggest that the physics of the ground state in the n-type copper-oxide superconductors differs from that in the p-type counterparts, which may be responsible for the strikingly different T_c they generated.

Finally, we discuss the nature of the superconducting gap. As seen in Fig. 2, $1/T_1$ in the superconducting (SC) state for H parallel to the CuO_2 -plane ($H \parallel a$ -axis) is reduced sharply just below T_c , and decreases in proportion to T^n upon further lowering T , with the exponent $n = 3$ for $6 \text{ K} \leq T \leq 13 \text{ K}$. As elaborated below, this is consistent with the existence of line-nodes in the SC order parameter. In terms of density of states (DOS), T_{1s} in the SC state is expressed as $\frac{T_{1N}}{T_{1s}} = \frac{2}{k_B T} \int \int (1 + \frac{\Delta^2}{E E'}) N_s(E) N_s(E') f(E) (1 - f(E')) \delta(E - E') dE dE'$, where $N_s(E)$ is the DOS in the SC state, $f(E)$ is the Fermi function, Δ is the energy gap. For an s-wave gap, $1/T_1$ should show a peak just below T_c due to the divergence of N_s at $E = \Delta$, and then decrease as $\sim \exp(-\Delta/k_B T)$. The broken curve in Fig. 2 is the calculated T -dependence of $1/T_1$ for the simple BCS gap which was applied previously to several n-type cuprates [24, 25, 26, 27]. By contrary, for a line-nodes gap such as d-wave gap, the peak just below T_c is removed [28], and a $N_s(E) \propto E$ at low E results in the $1/T_1 \propto T^3$ behavior at low temperatures. In the present case, the deviation of $1/T_1$ from T^3 at $T \leq 6 \text{ K}$ is explained as due to the presence of impurity (disorder) scattering which brings about a residual DOS (N_{res}) at the Fermi level (E_F) in the case of linenodes gap [29, 31]. Note that an anisotropic (or extended) s-wave gap model can not explain the T -linear behavior of $1/T_1$ at low T [31]. To demonstrate the result of line-nodes gap, we applied the $d_{x^2-y^2}$ gap model, $\Delta(\theta) = \Delta_0 \cos(2\theta)$, in the presence of disorder [29]. The calculation finds excellent agreement with the experimental data as seen in Fig. 2, with $2\Delta_0 = 3.8 k_B T_c$ and $N_{res} = 0.15 N(E_F)$. The same model can also consistently explain the Knight shift below T_c , for a choice of $K_{orb} = 0.155\%$, but the difference between the d-wave and the s-wave cases in the Knight shift result is generally small, which is also true in the present case. In summary, our results in the SC state are compatible with the photoemission and scanning SQUID experiments that found d-wave-like gap in $\text{Nd}_{1.85}\text{Ce}_{0.15}\text{CuO}_4$ [32, 33, 34].

In conclusion, from ^{63}Cu NMR measurements in an electron low-doped copper oxide superconductor $\text{Pr}_{0.91}\text{LaCe}_{0.09}\text{CuO}_{4-y}$, we find that no pseudogap shows up and that the low- T ($T \leq 55 \text{ K}$) spin dynamics is renormalized to well conform to the prediction for the Fermi liquid that persists as the ground state when the superconductivity is removed. This is the first case in which the normal state in the zero-temperature limit was investigated by a microscopic probe. The NMR data set in the superconducting state, which was obtained for the first time in $\text{Re}_{2-x}\text{Ce}_x\text{CuO}_4$, can be consistently explained by line-node gap model. These results shed light on understanding doped Mott insulators and superconductivity derived from them.

We thank H. Kohno, K. Miyake, M. Ogata, Z.-X. Shen, T. Tohyama, C. M. Varma, and T. Xiang for useful discussions, and Y. Okita for assistance in some of the mea-

surements. Support by MEXT grants Nos. 11640350, 14540338 (G.-q.Z), 13740216 (M.F) and 12046239 (Y.K and K.Y) is acknowledged.

-
- [1] L.D. Landau, Soviet Physics JETP **3**, 920 (1957).
 - [2] T. Timusk, B. Statt, B. Rep. Prog. Phys. **62**, 61 (1999).
 - [3] P. W. Anderson, Science **235**, 1196 (1987).
 - [4] Y. Tokura, H. Takagi, S. Uchida, Nature **337**, 345 (1989).
 - [5] H. Takagi, S. Uchida, Y. Tokura, Phys. Rev. Lett. **62**, 1197 (1989).
 - [6] J.L. Peng *et al*, Phys. Rev. **B 55**, 6145 (1997).
 - [7] R.W. Hill *et al*, Nature **414**, 711 (2001).
 - [8] J. Korriga, Physica **16**, 601 (1950).
 - [9] M. Fujita *et al*, Phys. Rev. **B 67**, 014514 (2003).
 - [10] G.-q. Zheng *et al*, J. Phys. Soc. Jpn. **58**, 1910 (1989); S. Kambe *et al*, J. Phys. Soc. Jpn. **60**, 400(1991). K. Kumagai *et al*, Physica **C 185-189**, 1073 (1991). T. Imai *et al*, J. Phys. Chem. Solids, **56**, 1921 (1995).
 - [11] J.L. Cooper, Phys. Rev. **B 54**, R3753 (1996).
 - [12] G.-q. Zheng *et al*, Phys. Rev. **B60**, R9947 (1999); Physica **C 364-365**, 485 (2001).
 - [13] G.-q. Zheng *et al*, Phys. Rev. Lett. **85**, 405 (2000).
 - [14] G.-q. Zheng *et al*, J. Phys. Soc. Jpn. **64**, 2524 (1995).
 - [15] A. Narath, Phys. Rev. **162**, 320 (1967).
 - [16] above $T=20 \text{ K}$, the anisotropy of T_1 is T -independent, with $\frac{T_1(H//c)}{T_1(H//a)}=3.3$.
 - [17] T. Moriya, J. Phys. Soc. Jpn. **18**, 516 (1963).
 - [18] A.J. Millis, H. Monien, D. Pines, Phys. Rev. **B 42**, 167 (1990).
 - [19] T. Moriya, K. Ueda, Y. Takahashi, J. Phys. Soc. Jpn. **59**, 2905 (1990).
 - [20] G.-q. Zheng *et al.*, Physica **C 208**, 339 (1993).
 - [21] C. M. Varma *et al.*, Phys. Rev. Lett. **63**, 1996 (1989). **64**, 497(E) (1990).
 - [22] This $K_{orb,a}$ and $K_{orb,c}=0.92\%$ are both smaller than the respective values in p-type cuprates (see for example Ref. [12]). This is consistent with the result of the very small ν_Q that indicates a reduced hole number in the $\text{Cu}3d$ orbit. Namely, $K_{orb,c} = n_{x^2-y^2} \frac{8\mu_B^2}{E_{xy} - E_{x^2-y^2}}$, where $n_{x^2-y^2}$ is the hole number in the $3d_{x^2-y^2}$ -orbit and the denominator is the energy difference between the two designated orbits [14].
 - [23] Y. Ando *et al*, Phys. Rev. Lett. **75**, 4662 (1995).
 - [24] Q. Huang *et al*, Nature, **347**, 369 (1990).
 - [25] B. Stadlober, G. Krug, R. Nemeschek, R. Hackl, Phys. Rev. Lett. **74**, 4911 (1995).
 - [26] J.A. Skinta *et al*, Phys. Rev. Lett. **88**, 207003 (2002).
 - [27] C.-T. Chen, *et al*, Phys. Rev. Lett. **88**, 227002 (2002).
 - [28] see *e.g.*, G.-q. Zheng *et al*, Phys. Rev. Lett. **86**, 4664 (2001).
 - [29] T. Hotta, J. Phys. Soc. Jpn. **62**, 274 (1993).
 - [30] L. C. Hebel, Phys. Rev. **16**, 79 (1959).
 - [31] R. Fehrenbacher and M. R. Norman, Phys. Rev. **B 50**, 3495 (1994).
 - [32] C.C. Tsuei and J.R. Kirtley, Phys. Rev. Lett. **85**, 182 (2000).
 - [33] T. Sato *et al.*, Science **291**, 1517 (2001).
 - [34] N.P. Armitage, *et al*, Phys. Rev. Lett. **86**, 1126 (2001).